Estimates of the rates of microstructural changes in mylonites

DAVID J. PRIOR[1], ROBERT J. KNIPE[2] & MARK R. HANDY[3]

[1] *Department of Earth Sciences, Liverpool University, Liverpool L69 3BX, UK*

[2] *Department of Earth Sciences, Leeds University, Leeds LS2 9JT, UK*

[3] *Geologisches Institut, Universität Bern, Switzerland*

Abstract: Microstructures developed during dislocation creep such as the dynamically recrystallized grain-size and the subgrain-size are modified in response to increasing differential stresses and shear-strain rates adjacent to rigid minerals in mylonites. In two specimens variations in quartz subgrain-size around rigid minerals has been quantified from orientation contrast SEM images. In a deformed granite from the Pogallo ductile fault zone, quartz two-dimensional subgrain-size is reduced from background values of about 30 μm to 8 μm and then 4 μm in progressively narrower channels between rigid feldspars. In pelitic mylonites from the Alpine fault zone, New Zealand, quartz bands are wrapped around rigid garnets and the subgrain-size is reduced from background values of about 20 μm to 14 μm within 2000 μm of the garnet to 11 μm adjacent to the garnet. In both specimens examined the microstructure responds to both increases and decreases in differential stresses and coupled strain-rates. The analysis of the distribution of subgrain sizes provides information for the assessment of microstructural stability and the estimation of the rates of microstructural changes. The New Zealand specimens have good regional shear strain-rate controls and minimum subgrain boundary migration rates (during reduction in differential stresses and strain-rates) of 1.2×10^{-9} μm s^{-1} to 1.2×10^{-11} μm s^{-1} are estimated, for bulk shear strain rates of 10^{-10} s^{-1} and 10^{12} s^{-1} respectively. Palaeopiezometry coupled with rheological considerations suggests that these microstructural changes correspond to minimum differential stress-rates of 5×10^{-9} MPa s^{-1} to 5×10^{-11} MPa s^{-1}. Similar or slower regional stress-rates during fault zone evolution, will allow continuous re-equilibration of the microstructure. Thus the time at which any given microstructure is frozen in will be critically dependent upon fault zone deformation history. In the Alpine fault zone rapid uplift and high near surface temperatures combine to generate rapid stress drops as mylonitic deformation gives way to cataclastic faulting during uplift. Mylonite microstructure is frozen in during this rapid stress drop and represents the shallowest level of major crystal-plastic deformation.

Quantification of microstructural stability, specifically the rates at which microstructures are modified due to changes in conditions of stress, strain rate, temperature, depth and fluid composition and activity, is essential if microstructures are to be used to evaluate dynamic processes in the Earth's crust (Knipe 1989). This paper examines one aspect of microstructural stability; the microstructural response of quartz mylonites to changing differential stress and strain-rate conditions.

Quartz mylonites often contain a dynamic equilibrium microstructure (Bell & Etheridge 1973) which can be used to evaluate the kinematics, differential stresses and strain-rates of deformation. Constitutive flow laws for dislocation creep (see Handy 1989; Paterson & Luan, this volume) indicate an interdependence of differential stress and strain rate which cannot be decoupled. For deformation accompanied by dynamic recrystallization, the grain-size and subgrain-size are related to differential stress levels (Twiss 1977, 1986) and coupled strain-rates for a given temperature of deformation. This relationship is documented for quartz in experiments and in natural examples (Mercier *et al.* 1977; Christie *et al.* 1980; Ord & Christie 1984). If conditions of deformation are changing, as might be expected in an uplift path, then it is important to be able to assess whether the observed microstructure developed during the last increments of strain, at the peak stress condition or during some other time period. Recent analysis of mylonite evolution has recognised the importance of cyclic changes in the microstructure (White *et al.* 1980; Means 1981; Knipe 1989). The differential stress and strain-rate fields within a mylonite are likely to be inhomogenous (Lister & Price 1978; Masuda & Ando 1988) and there is a need to identify situations where the influence of changing stress and strain-rate conditions on microstructural

From Knipe, R. J. & Rutter, E. H. (eds), 1990, *Deformation Mechanisms, Rheology and Tectonics*, Geological Society Special Publication No. 54, pp. 309–319.

evolution can be assessed. One such situation is in the proximity of rigid particles. As matrix material flows around and past such particles it experiences an increase followed by a decrease in differential stress and in strain-rate (e.g. Masuda & Ando 1988; Handy 1990). If the geometrical evolution can be modelled and the bulk strain-rates estimated, in these situations, then the rate of microstructural change associated with local changes in differential stress and strain-rates can be constrained. These data can then be applied to large-scale changes in differential stress and strain-rate to infer how mylonitic microstructures will respond to fault zone evolution and changing deformation conditions.

Microstructural environments around rigid phases in mylonites

Mylonites containing phases which behave rigidly are well documented (Boullier 1980; Lister & Price 1978; Mitra 1978; Price 1978; White *et al.* 1980; White 1984). A rigid body in a viscous material will cause a localized perturbation in the differential stress field and strain-rate pattern (Masuda & Ando 1988). In granitic and metasedimentary mylonites; feldspars, garnet, zircon, amphiboles and ore phases usually act as rigid particles and cause the strain in the surrounding matrix (quartz and mica) to accommodate this incompatibility (Lister & Williams 1983; Lister & Price 1978). The microstructure adjacent to these particles may be modified in response to changing differential stress, strain-rate and strain field conditions with or without a change in the dominant deformation mechanism. Such modifications include reduction of the quartz grain and subgrain-sizes in regions adjacent to the rigid bodies (Etheridge & Wilkie 1979; Lister & Price 1978). Knowledge of the flow lines for material around a rigid object combined with constraints on the shear strain rate can be used to quantify the rate at which the material moves around the localized differential stress and strain-rate field of a rigid body. These data coupled with analysis of the quartz microstructures along the flow lines around rigid bodies facilitate quantification of the rates of microstructural change in response to the changing differential stresses and strain-rates.

Changes in quartz microstructure around rigid objects have been investigated in two mylonites: (a) the deformed San Rocco Granite from the Pogallo ductile fault zone, southern European Alps (Handy 1986), and (b) the Alpine fault mylonites, South Island, New Zealand (Sibson *et al.* 1979; Prior 1989). These two examples provide contrasting local differential stress/strain-rate environments and are discussed separately below.

Methods

Specimen blocks were polished to better than 3 μm surface roughness using diamond abrasive on a cloth lap and then put onto a Malvern Instruments Multipol 2 mechanical/chemical polisher (Fynn & Powell 1979; Lloyd 1987) using a polyeurethane lap and SYTON fluid for 4 to 10 hours. Specimens were examined on a Camscan Series 4 scanning electron microscope (SEM) in orientation contrast mode (Lloyd 1987) using a working distance of 7–8 mm, an accelerating voltage of 30 kV and a beam current of 175 nA. Distinct boundaries with lattice rotations > 0.25° can be imaged by this method with sub-micrometre spatial resolution, so that this technique is ideal for imaging subgrains. However it must be emphasized that the change in BSE grey level across a boundary is not simply a function of mis-orientation, so that a 0.25° boundary, a 5° boundary or any other arbitrary boundary mis-orientation are not readily distinguishable without systematic collection of electron channelling patterns (ECPs) from each subgrain (Lloyd 1987). The term subgrain in this paper will always refer to the smallest crystallographic units observed in orientation contrast SEM.

Locating micrographs were taken at 10× to 100× magnification. Micrographs to be used for quantification of subgrain-sizes were all taken at the same magnification in any one given specimen (usually between 500× and 1500×). Areas comprised of pure quartz, as close to an assumed flow line around the rigid object as possible, were chosen for subgrain-size measurement. Where possible ECPs were used to assess typical boundary mis-orientations. Two dimensional subgrain areas (A) were quantified using a digitizing tablet. Two dimensional subgrain-size (d) is calculated as the diameter of a circle of equivalent area (A) to the measured grain. Three dimensional subgrain-size (D) is estimated using the linear stereological correction $D = 4d/\pi$ (Exner 1972). Mean subgrain-sizes and corresponding standard deviation are calculated assuming $\sqrt{d}$ is normally distributed. Because standard deviations are calculated from the $\sqrt{d}$ distribution corresponding errors in d are asymmetrically distributed.

Quartz subgrain-size around feldspars in deformed San Rocco Granite

The Permian San Rocco granite was variably deformed in the Pogallo ductile fault zone under greenschist facies conditions (PDFZ: Handy 1986). Quartz crystallographic fabrics indicate a significant component of simple shear deformation predominated in the PDFZ although shape analyses of quartz ribbons indicate K

values mainly between 0.3 and 0.4. Optical estimates, in transmitted light, of the mean two dimensional dynamically recrystallized quartz grain-sizes of 20 μm to 40 μm suggest differential stresses during deformation of 30 MPa to 50 MPa (using the theoretical recrystallized grain-size palaeopiezometer of Twiss 1977). Rheological considerations bracket shear strain rates between $10^{-8}s^{-1}$ and $10^{-13}s^{-1}$ but shear strain rates are only poorly constrained independently of microstructural criteria.

One specimen of the San Rocco Granite (HD47), cut parallel to lineation, is examined in detail here. The quartz is 100% dynamically recrystallized but its microstructure is different in the areas of constricted flow and pressure shadows created by feldspars 1–5 mm in size. The feldspars have undergone minor fracturing and associated sericitization but have not accommodated significant strain. Flow stresses, estimated from optical measurements of quartz recrystallized grain-size, are amplified by a factor of 2–3 in constrictions relative to pressure shadows (Handy 1990).

An orientation contrast BSE montage of a constriction in which subgrain-sizes have been estimated is shown in Fig. 1. Quartz flow is constrained between a rounded feldspar (*c.* 400 μm radius) and a large flat feldspar. A few millimetres to the right of the imaged area the quartz band thickens to *c.* 1 mm and has a mean subgrain-size in excess of 30 μm. The entire imaged region is a constriction with significantly reduced subgrain-size. The two dimensional subgrain-size is reduced to 8.0 μm [+4.7 −3.6] (mean of cumulated data from areas 1, 4, 5, 6 and 7 in Fig. 1) across most of the imaged area and to 4.5 μm [+1.9 −1.5] (mean of cumulated data from areas 2 and 3 in Fig. 1) in an anvil shaped region above the apex of the rounded feldspar. There is a 40 μm thick arc marginal to the apex of the lower feldspar where subgrain-size is not reduced although there are not enough clearly defined grains in this region for subgrain-size quantification. The microstructural transition into the anvil shaped region is sharp ($\leq$ 10 μm thick) up to 80 μm to 100 μm from the round feldspar, but then widens to an ill-defined transition (over 100 μm to 200 μm) adjacent to the overlying flat faced feldspar (Fig. 1).

Quartz subgrains across the majority of the imaged area are subhedral with axial ratios between 1:1 and 2:1. There are local boundary alignments; broadly top left to bottom right in Fig. 1. Most subgrain boundaries are irregular with serrations of amplitude 1 μm to 5 μm. Subgrain boundary intersections commonly define a 120° dihedral angle. In many cases the 120° angle is only maintained within a few micrometres of the intersection. In the region containing the smaller subgrains there are more euhedral and equant subgrains. Although approximately 25% of subgrains have straight boundaries, the majority of boundaries are serrated, indicating that some subgrain boundary migration has taken place. Subgrain-size histograms (Fig. 1) show that the small fraction which dominates the anvil shaped region also form a significant proportion of the size fraction across the rest of the imaged area. The subgrain-size transition is accommodated by the loss of the broad tail of coarser grains. Crystallographic orientations have not been systematically investigated in specimen HD47 but optical observations indicate that there are strong preferred *c*-axis orientations which are maintained through reduced grain-size regions in flow constrictions. A detailed study of crystallographic preferred orientations (CPO) in other San Rocco Granite specimens shows that constricted regions have strong CPOs but these are distinct from the CPO of pressure shadows (Handy 1990).

Quartz grain-size around garnets in the Alpine fault mylonites

The Alpine fault mylonites (Sibson *et al.* 1979; Prior 1989) developed during Alpine fault motion which probably started no earlier than 22 Ma (Carter & Norris 1976; Kamp 1986). Kinematic indicators (Prior 1989) show that the deformation developed during the transpressive phase of simple shear motion which started about 5 Ma ago (Walcott 1984). Deformation is dominated by simple shear and regional criteria constrain the bulk shear strain rate across the 1 km wide mylonite zone at between 10^{-13} s^{-1} to 10^{-11} s^{-1}. Often an early mylonitic foliation is truncated by a later mylonitic foliation. Kinematic indicators always show that both foliations developed during the same sense of bulk shear. These data suggest that shearing within the Alpine fault mylonites at any one time was restricted to a zone considerably thinner than the total thickness of mylonites. In individual sections which cross the entire width of the mylonites there are typically between 10 and 30 such truncations of one fabric by another. Thus, to account for the localization of mylonitic deformation at any one time the shear strain rate estimates must be increased by at least an order of magnitude to 10^{-12} s^{-1} to 10^{-10} s^{-1}. These estimates are conservative,

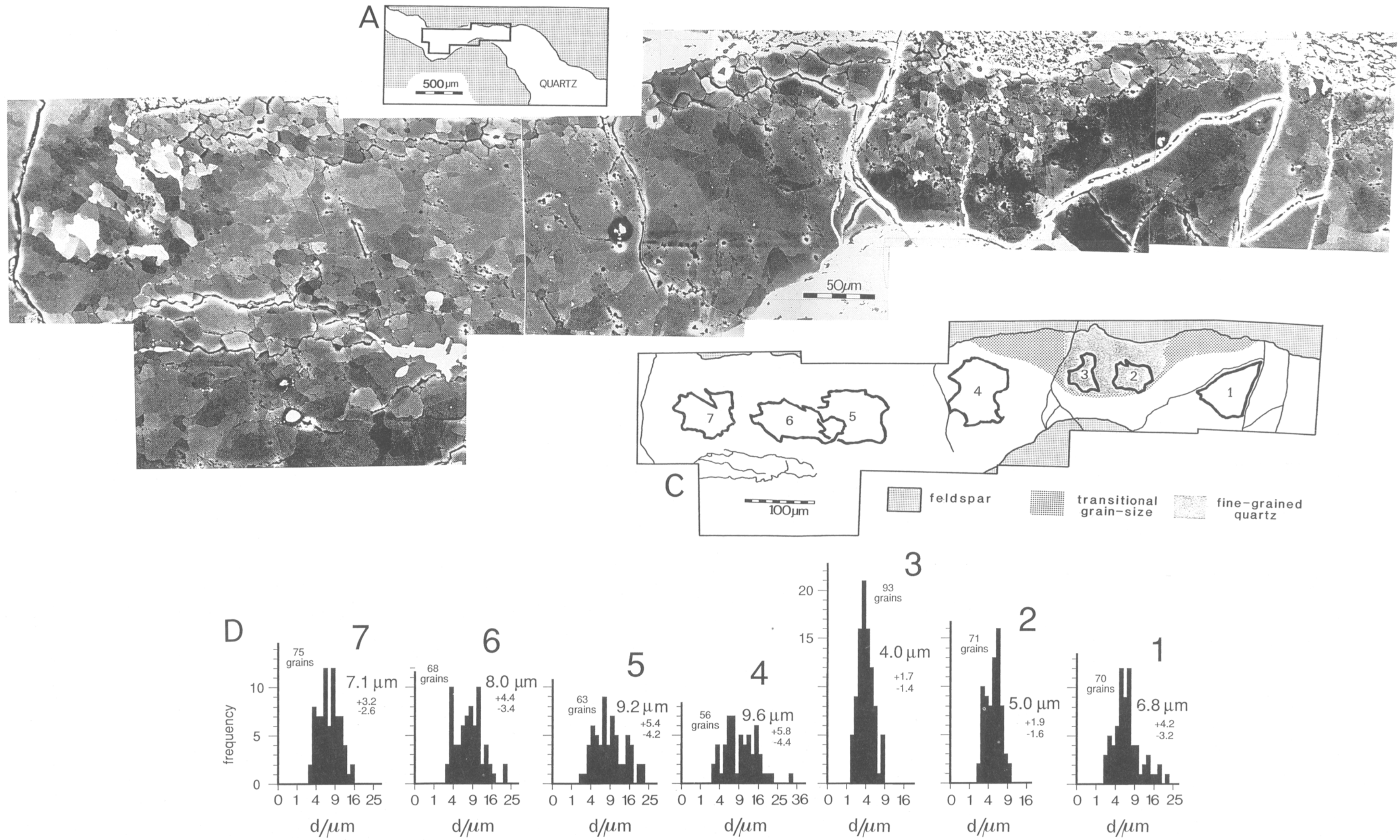

Fig. 1. Microstructure between two feldspars in a specimen of deformed San Rocco Granite (HD47) from the Pogallo ductile fault zone of the southern European Alps. (**A**) Location sketch, traced from a BSE micrograph. Box shows the area examined in detail on the SEM and illustrated in (B) and (C). (**B**) Montage of BSE orientation contrast micrographs showing the constriction of quartz located in (A). Apart from obvious cracks all contrast in the quartz relates to differences in crystallographic orientation. (**C**) Sketch, traced from the montage shown in (B), to locate subgrain-size analysis areas 1 to 7 and to highlight the reduced subgrain-size in the region above the apex of lower rounded feldspar. This anvil shaped region comprises a core of fine-grained quartz and a transitional boundary of variable thickness (see text). Cracks are marked to help location relative to (B). (**D**) Subgrain-size (plotted so that $\sqrt{d}$ is linear) versus frequency histograms for areas 1 to 7. Each plot shows the subgrain-size equivalents of the mean and standard deviation of the $\sqrt{d}$ distribution. Data are not stereologically corrected.

shear strain rates are probably faster than these. Optical estimates in transmitted light of two dimensional dynamically recrystallized quartz grain-sizes of 18 μm away from the rigid particles suggests differential stresses during deformation of 30 MPa to 70 MPa, using the Twiss, (1977) palaeopiezometer (by D. C. Green in 1982; Prior 1989). Mean subgrain-sizes, from orientation contrast SEM images, in regions remote from rigid particles vary from 18 μm to 26 μm.

The mylonite contains phases, including garnet, which developed in the much older Rangitata metamorphism (Landis & Coombs 1967) and are now porphyroclasts. Garnets have not accommodated significant strain although they are affected by fracturing and associated retrogression. The distinctive quartz bands are thinner adjacent to garnets and grain-size reduction in the thinned regions can be observed optically.

Specimen DC3A, from Darnley Creek, a tributary of the Waitangi–Taona river north of Waiho, has been studied in detail. This specimen was cut parallel to the regionally and locally defined movement direction (± 10°) and perpendicular to foliation. The shear sense is clearly

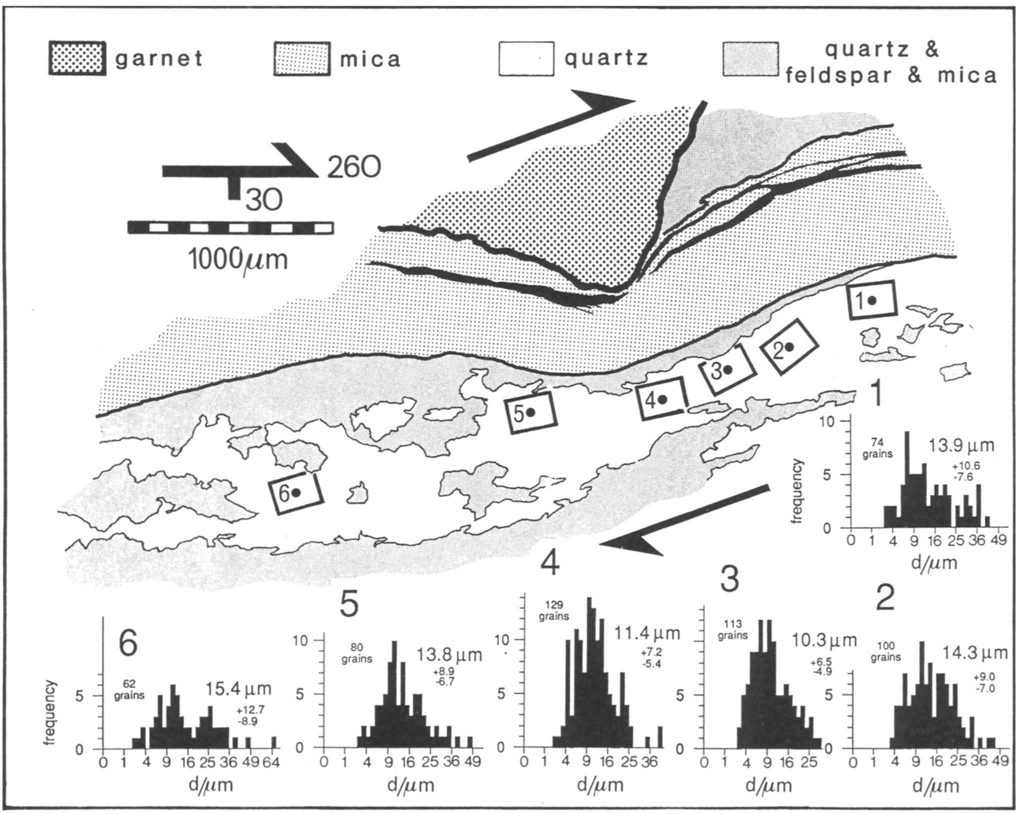

Fig. 2. Microstructure of a quartz band buckled around a garnet in a sample (DC3A) from the Alpine fault mylonites, South Island, New Zealand. Orientation mark relates to the geographical reference frame. Shear sense indicators are based on data from this and neighbouring specimens and are consistent with regional movement senses. The specimen surface is parallel to the movement direction and perpendicular to foliation. A lower magnification sketch of this region is shown in Fig. 4. Some parts of the quartz band contain feldspar and mica impurities. These areas (shaded) are distinguished from pure quartz (no ornament). Numbered boxes show the locations of orientation contrast BSE images used to generate the subgrain-size data. Numbered subgrain size (plotted so that $\sqrt{d}$ is linear) versus frequency histograms 1 to 6 correspond to location boxes 1 to 6. Each plot shows the subgrain-size equivalents of the mean and standard deviation of the $\sqrt{d}$ distribution. Data are not stereologically corrected.

defined by shear bands, asymmetrical microfolds and mica fish in this and neighbouring specimens. Only one of three garnets examined is wrapped by a quartz band sufficiently pure to allow subgrain-size analysis of *c.* 100 grains. A line drawing of the area examined and the subgrain-size data measured in this region is shown in Fig. 2. Flow paths are assumed to be parallel to foliation, here defined by the boundary of quartz/quartz–feldspar–mica bands and mica bands. Five measurements areas (1 to 5) were selected along an interpreted particle flow path which is at its closest 0.6 mm from the garnet margin (2.1 mm from the garnet centre). A sixth measurement (area 6) is not along the same flow path because of the presence of feldspars and is located on a flow path approximately 0.3 mm further from the garnet. Parts of the orientation contrast BSE images used to quantify subgrain-sizes for areas 2 and 3 are shown in Fig. 3. Two dimensional subgrain-size is reduced from measured background values averaging 14.3 μm [+10.1 −7.4] (mean of areas, 1, 2, 5, & 6) to 10.9 μm [+6.9 −5.2] (mean of areas 3 & 4) in the region closest to the garnet. All the areas examined here have subgrain-sizes less than far-field subgrain-size estimates of 18 μm to 26 μm. Subgrain-size histograms (Fig. 2) show that the regions with smaller subgrains contain the same overall range of sizes as the coarser areas but the frequency distribution is altered.

The microstructure of the coarse and fine subgrain regions is similar. Subgrains are euhedral to subhedral with axial ratios from 1:1 to 4:1. About 30% of subgrain boundaries are straight, the others have serrations of amplitude 5 μm to 10 μm. Grain modification occurs by a

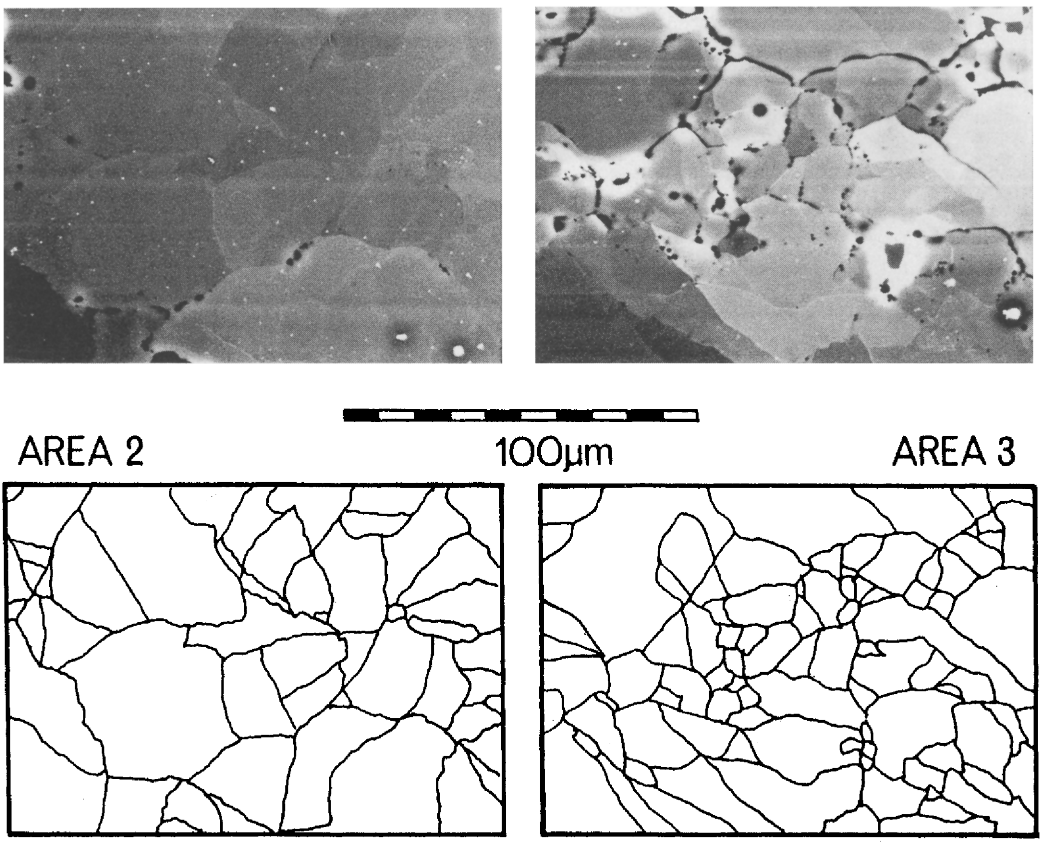

Fig. 3. Part of the BSE orientation contrast micrographs of areas 2 and 3 in Fig. 2. and line drawings of the subgrain boundaries for the same areas.

combination of subgrain rotation recrystallization and grain boundary migration (Prior 1988). ECPs show that a significant number of the subgrain boundaries imaged (from a random sample of about 10) have misorientations of a few degrees, and that very low angle (> 1°) boundaries are rare.

Microstructural stability

In both the mylonites studied the microstructures present arise from the operation of dynamic recrystallization during dislocation creep. There is a well defined decreases in the subgrain-size adjacent to the feldspar and garnet grains studied. This decrease is produced as quartz grains move into the differential stress and strain-rate perturbation adjacent to the rigid particle and from the microstructures preserved probably involves the generation and misorientation of new dislocation walls in addition to subgrain wall migration. It is not possible to assess the relative importance of these two processes during this subgrain-size decrease. The subgrain-size increase which takes place as material flows away from the rigid particle is likely to be controlled by subgrain wall migration.

Edward *et al.* (1982) show that the subgrain-size stress relationship may be perturbed by environmental parameters such as temperature and fluid activity. Temperature must have been constant across the few mm of specimens observed in this study. Fluid activity may vary locally in the vicinity of porphyroclasts of feldspar or garnet (Wintsch & Knipe 1983; Wheeler 1987). However quartz subgrain-size does not vary adjacent to small feldspar and garnets (those the same size as the quartz grains) suggesting that it is the increase in differential stress and strain-rate around relatively large rigid bodies which are the prime control on the local quartz subgrain size.

The data presented in this paper show clearly that the subgrain-size and the recrystallized grain-sizes preserved in mylonites do not necessarily preserve the peak differential stress conditions experienced. Subgrain and grain-sizes can respond to both increases and decreases in differential stress and strain-rate. The microstructures recorded reveal that differential stress and strain rate variations expected during deformation of material containing rigid particles are preserved. However, large scale readjustment of the microstructure after deformation, which would remove such grain-size and subgrain-size variations, has not taken place. The time at which the subgrain sizes have been frozen in is likely to be critically dependent upon the rates of change of deformation conditions (Knipe 1989).

Experimental data (Ross *et al.* 1980) shows that olivine subgrain sizes respond to increases in differential stress and strain rate but not to stress relaxation. Similarly experiments in polycrystalline Mg (White *et al.* 1985) show that peak recrystallized grain-sizes can be preserved. These data contrast with our observation that microstructural change does occur in natural stress relaxation. The conflicting data may reflect different materials and stress relaxation rates. The data presented in this paper are consistent with dynamic models of subgrain development in which subgrain-size is reduced by the formation of new boundaries and may increase by the mobility and mutual annihilation of boundaries (Takeuchi & Argon 1976; Edward *et al.* 1982; Poirer 1985) with substructure modification by the creep of individual dislocations within subgrains and subgrain boundaries. Such models reflect the realistic continuum of processes linking recovery and recrystallization.

There is sufficient geometrical and shear strain rate information to assess the stability of the microstructures and in the case of the Alpine Fault mylonites to estimate the rates at which the microstructural changes take place. Although the shear strain rate is amplified in the constricted region adjacent to the garnet (the magnitude of this increase is estimated later) the mean shear strain rate of the constricted region and the area encompassing the garnet, which does not deform, must be equivalent to the bulk strain-rate. Thus the time taken for flow along a flow line around the garnet can be approximated using the bulk shear strain rate. Figure 4 shows the geometrical model applied to calculate the time it has taken the quartz now at areas 5, 4, 3 and 2 to travel from a position relative to the garnet equivalent to the location of area 1 (see Fig. 2 to locate these areas). In each case the bulk shear strain, relative to a base line bisecting the garnet and parallel to the flow plane, involved in translating from locality one is calculated (Fig. 4) and the time taken estimated using the regional shear strain rate constraints.

The mean subgrain-size of areas 1, 2, 5 and 6 (14.3 μm: Fig. 5) is taken as the background subgrain-size and the mean subgrain-size of areas 3 and 4 (10.9 μm: Fig. 5) is taken for the high stress region adjacent to the garnet. These give a change in two dimensional subgrain-size (d) of 3.4 μm and a change in stereologically corrected three dimensional subgrain-size (D)

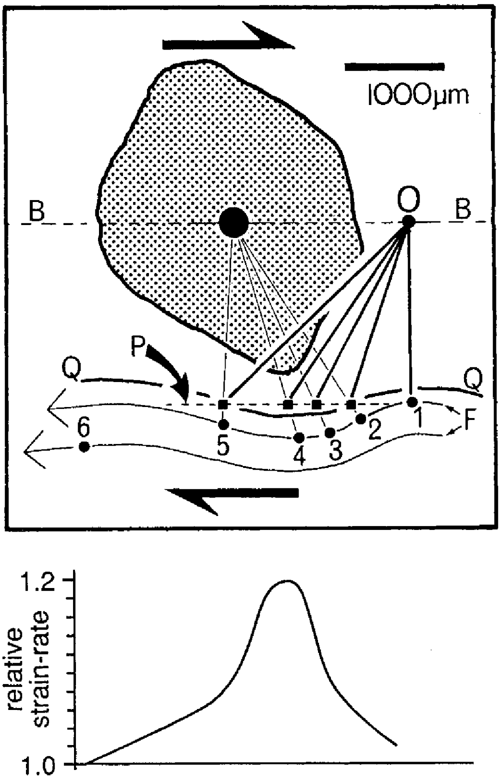

Fig. 4. Geometrical construction used to calculate the bulk shear strain associated with the flow of material from area 1 to areas 2, 3, 4, and 5 in the Alpine fault mylonite specimen. Sketch is traced from a BSE micrograph. Q–Q marks the edge of the quartz band (see Fig. 2). Garnet is stippled. Shear strains are calculated as the change in angle between a baseline (B–B), parallel to foliation and passing through the garnet centre, and a line perpendicular to this and passing through area 1. To make these calculations the deflecting effects of the garnet on particle flow paths (F) must be removed. Deflection due to the garnet is assumed to be radial from the garnet centre. Correction is made by projecting areas 2 to 5 along radial lines onto an 'undisturbed' particle path (P) constructed using the undeflected foliation orientations to the left and right of the image. The bulk shear strain involved in particle translation from area 1 to area 2 is given by tan (O_1 ^OP_2) where P_2 is the projection of 2 onto line P. Similar equations are used for areas 3 to 5. The lower graphs shows the shear-strain rate of points in the constriction relative to the shear strain-rate at locality 6. These data are calculated from the ratio of the flow line separation at each point and locality 6.

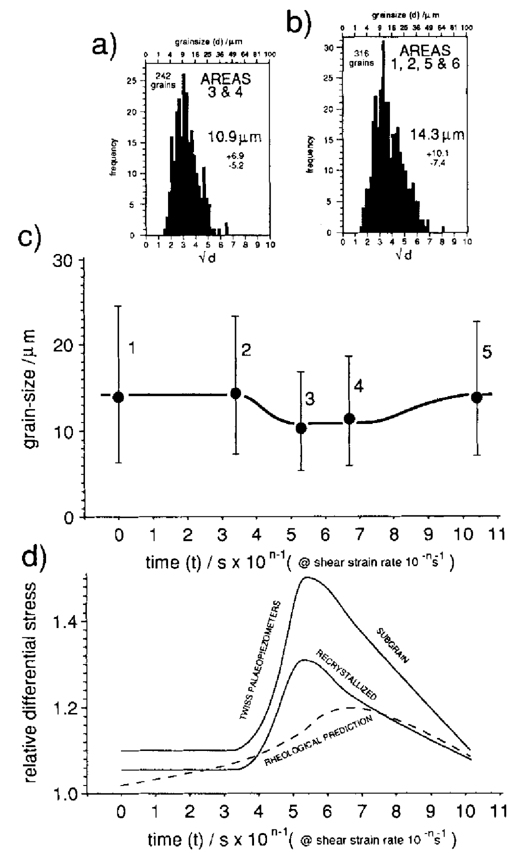

Fig. 5. Cumulation of subgrain-size data and interpretive subgrain-size time relationships for the flow of quartz around garnet in the Alpine fault mylonite specimen (Fig. 2). (**a**) Root subgrain-size ($\sqrt{d}$ in μm) versus frequency histogram for quartz close to the garnet margin (areas 3 & 4). (**b**) Root subgrain-size ($\sqrt{d}$ in μm) versus frequency histogram for background quartz (areas 1, 2, 5 & 6). Histograms show the subgrain-size equivalents of the mean and standard deviation of the $\sqrt{d}$ distribution. Data are not stereologically corrected. (**c**) Graph of subgrain-size (spots show mean and vertical bars standard deviation of the $\sqrt{d}$ distribution) for areas 1 to 5 (see Figs 2 & 4) against the time calculated for flow from area 1 to each of these areas. (**D**) Graphs showing estimates of differential stresses relative to the differential stress at measurement point 6 calculated from two palaeopiezometers and from rheological considerations (see text).

of 4.3 μm. This decrease in the subgrain-size is fully accomplished between areas 2 and 3, indicating a maximum time of 1.9×10^9 s at a shear strain rate of 10^{-10} s^{-1} or 1.9×10^{11} s at a shear strain rate of 10^{-12} s^{-1}. The minimum rate of change in subgrain-size during increasing stress is calculated (for stereologically corrected data) at 2.3×10^{-9} μm s^{-1} (71500 μm Ma^{-1}) at a shear strain rate of 10^{-10} s^{-1} or 2.3×10^{-11}

μm s^{-1} (715 μm Ma^{-1}) at a shear strain rate of 10^{-12} s^{-1}. This transition occurs during increasing differential stress and strain-rate and reflects the period needed to establish the new microstructure. The equivalent change during decreasing differential stress and strain-rate occurs between areas 4 and 5 and may take twice as long as the up-stress transition although this would be a maximum value since there are no data points between 4 and 5. If, as is likely, this increase in the subgrain-size is controlled by subgrain boundary migration then the minimum net rate of subgrain boundary migration will be equivalent to the rate of change in subgrain-size (between areas 4 and 5) and is calculated (for stereologically corrected data) at 1.2×10^{-9} μm s^{-1} (36700 μm Ma^{-1}) at a shear strain rate of 10^{-10} or 1.2×10^{-11} μm s^{-1}

The rates of microstructural changes calculated here are conservative. The shear strain rates used are minima and the transition in grain-size may occur in only part of the time in the transition time interval. In addition the rates of subgrain migration calculated relate to the net effect of boundary migrations rather than the rate of migration of individual boundaries. Since the microstructure is dynamic, subgrain boundary migration is likely to be occurring to both increase and decrease grain-sizes and the mean rate will be slower that for any individual boundary.

The amplification of shear-strain rate in the constricted region around a rigid body can be estimated from the changing separation of flow lines. The shear-strain rate pattern around the garnet is shown in Fig. 4. By application of a flow law for quartz to the shear-strain rate amplification pattern the differential stress amplification can also be estimated. The differential stress amplification around the garnet is estimated using Paterson de Luan's (this volume) preferred stress exponent of 4 (Fig. 5D). Absolute differential stress magnitudes and amplifications can be estimated by the application of palaeopiezometers to subgrain-size data. The differential stress amplifications calculated using the subgrain and recrystallized grain size palaeopiezometers of Twiss (1977; 1986) are shown in Fig. 5D. The differential stress amplification curve for the recrystallized grain-size palaeopiezometer fits the curve calculated from rheological considerations much more closely than the data from the subgrain palaeopiezometer suggesting, albeit tentatively, that the recrystallized grain-size palaeopiezometer gives more realistic results here. Using the recrystallized grain-size palaeopiezometer (Twiss 1977) the differential stress magnitude calculated for the cumulated, stereologically corrected subgrain-size data of the background region (localities 1, 2, 5 and 6) is 84 MPa [+54 −26] and that for the constriction around the garnet (areas 3 and 4) is 101 MPa [+56 − 29]. These data give differential stress rates during increasing stress of 9×10^{-9} MPa s^{-1} at a bulk shear strain rate of $10^{-10}s^{-1}$ and 9×10^{-11} MPa s^{-1} at 10^{-12} s^{-1}. Similarly differential stress rates during decreasing stress are estimated at 5×10^{-9} MPa s^{-1} at a bulk shear strain rate of $10^{-10}s^{-1}$ and 5×10^{-11} MPa s^{-1} at $10^{-12}s^{-1}$.

In the case of the Alpine fault mylonites the rate of change of the differential stress at the end of the dislocation creep deformation must have been faster than 5×10^{-9} MPa s^{-1} to 5×10^{-11} MPa s^{-1} which is the estimated stress rate range which did allow adjustment of the microstructure during flow around the rigid particle. These results compare well to theoretical predictions of Knipe (1989) which suggest that at 400°C differential stress must drop at a rate faster than 10^{-10} MPa s^{-1} to prevent the subgrain-size maintaining equilibrium with the changing stress conditions.

If the calculated rates of subgrain boundary migration during decreasing stress can be applied to dynamic equilibrium changes at uniform stress then an estimate of quartz microstructural recycling times in the Alpine fault mylonites can be made. For a 20 μm mean subgrain-size (d) the minimum time required to grow a 20 μm subgrain, which will be equivalent to the time needed to recycle the microstructure, will be 540 years and 54000 years at shear strain-rates of 10^{-10} s^{-1} and 10^{-12} s^{-1} respectively using the rates calculated for decreasing differential stress and strain rate. These estimated microstructural recycling times are considerably less than the 1−2 Ma required (Wellman 1979) for uplift from the maximum burial depth of *c.* 20 km (Cooper 1980) suggesting that subgrain sizes will maintain equilibrium with fault zone differential stresses and strain rates as they deform during an uplift path from the middle crust to shallow levels. The uplift rate associated with the Alpine Fault Zone is rapid, >10 mm Ma^{-1} (Wellman 1979), and the thermal model of Koons (1987) indicates that the temperatures needed for crystal plastic deformation (300−400°C) may be present within a few kilometres of the surface. Both these features indicate that deformation after the crystal plastic straining and mylonite formation will be short lived and this enhances the chances of preserving the deformation microstructures characteristic of the last stages of dislocation creep. In the final stages of uplift rapid temperature reduction allows major displacement to be accommodated by cataclastic processes and the associated stress drop freezes in the mylonite microstructure.

Similar rapid stress drops and high differential stress and strain-rate gradients in the wall rocks adjacent to active shear zones may have preserved the quartz microstructures in the PDFZ. This crustal scale shear zone was a km wide low angle extensional fault within a hot, uplifting and extending segment of the deep crust (Handy 1986). Amphibolite facies mylonites grade successively into greenschist facies mylonites and cataclasites at the contacts with intermediate depth crustal rocks and the preservation of this zonation of dynamic microstructures is attributed to the very high cooling rates and/or stress drops during the final stages of highly localized deformation.

The rates of microstructural change which we have estimated here provide some constraint with which to assess the period of shear zone evolution a given set of quartz microstructures may represent. In a given shear zone the age of preserved mylonite microstructures will be critically dependent upon the mylonite temperature-differential stress-strain rate history as well as the temperature and strain-rate dependencies of creep of the minerals in the mylonite. As a generalization, slow changes in deformation conditions, particularly differential stress and strain-rate, will favour continuous microstructural re-equilibration, whilst faster changes will allow the microstructure to be frozen in. Microstructures formed under high temperature, deep crustal conditions will require rapid uplift and cooling to avoid equilibration with stresses at shallower levels. This is only possible if the deformation is partitioned into weaker shear zones. Since mechanisms of microstructural recovery are thermally activated, decreasing temperatures during uplift favour higher localized stresses and so tend to increase stress and strain partitioning on all scales.

Work in the Alpine fault mylonites was initiated as part of a NERC studentship to D. J. P. at the University of Leeds. M. R. H. acknowledges support of the Swiss NSF (project 2971–0.88). Staff of the Westland National Park, were most helpful during fieldwork. We thank T. Masuda and E. Rutter for useful discussions in the developmental stages of this work, an anonymous reviewer for helpful comments and B. Smith for a particularly rigourous and perceptive review. SEM work benefitted from the advice of G. Lloyd, J. Harrington and T. Nichells. L. Miralles is thanked for help with collection of digitized data.

References

Bell, T. H. & Etheridge, M. A. 1973. Microstructure of mylonites and their descriptive terminology. *Lithos*, **6**, 337–338.

Boullier, A. M. 1980. A preliminary study of the behaviour of brittle minerals in a ductile matrix: example of zircon and feldspars. *Journal of Structural Geology*, **2**, 211–217.

Carter, R. M. & Norris, R. J. 1976. Cainozoic history of Southern New Zealand: an accord between geological observations and plate tectonic predictions. *Earth and Planetary Science Letters*, **31**, 85–94.

Christie, J. M., Ord, A. & Koch, P. S. 1980. Relationship between recrystallized grain-size and flow-stress in experimentally deformed quartzite. *Transactions of the American Geophysical Union*, **61**, 377.

Cooper, A. F. 1980. Retrograde alteration of chromian kyanite in metachert and amphibolite whiteschist from the Southern Alps, New Zealand, with implications for uplift on the Alpine Fault. *Contributions to Mineralogy and Petrology*, **75**, 153–164.

Edward, G. H., Etheridge, M. A. & Hobbs, B. E. 1982. On the stress dependence of subgrain size. *Textures and microstructures*, **5**, 127–152.

Etheridge, M. A. & Wilkie, J. C. 1979. Grainsize reduction, grain boundary sliding and the flow strength of mylonites. *Tectonophysics*, **58**, 159–178.

Exner, M. E. 1972. Analysis of grain and particle size distribution in metallic materials. *International Metallurgical Reviews*, **17**, 25–42,

Fynn, G. W. & Powell, W. J. A. 1979. *The cutting and polishing of electro-optic materials*. Adams Hilger, London.

Handy, M. R. 1986. *The structure and rheological evolution of the Pogallo Fault Zone. A deep crustal dislocation in the Southern Alps of northwestern Italy*. PhD thesis, Basel.

—— 1989. Deformation regimes and the rheological evolution of fault zones in the lithosphere: the effects of pressure, temperature, grainsize and time. *Tectonophysics*, **163**, 119–152.

—— 1990. The solid state flow of polymineralic rocks. *Journal of Geophysical Research*, **95**, 8647–8661.

Kamp, P. J. 1986. Late Cretaceous – Cenozoic tectonic development of the southwest Pacific region. *Tectonophysics*, **121**, 225–251.

Knipe, R. J. 1989. Deformation mechanisms, recognition from natural tectonites. *Journal of Structural Geology*, **11**, 127–146.

Koons, P. O. 1987. Some thermal and mechanical consequences of rapid uplift: the example of the Southern Alps, New Zealand. *Earth and Planetary Science Letters*, **86**, 307–319.

Landis, C. A. & Coombs, D. S. 1967. Metamorphic belts and orogenesis in southern New Zealand. *Tectonophysics*, **4**, 501–518.

Lister, G. S. & Price, G. P. 1978. Fabric development in a quartz feldspar mylonite. *Tectono-*

physics, **49**, 37–38.

—— & WILLIAMS, P. F. 1983. The partitioning of deformation in flowing rock masses. *Tectonophysics*, **92**, 1–33.

LLOYD, G. E. 1987. Atomic number and crystallographic contrast images with the SEM: A review of backscattered techniques. *Mineralogical Magazine*, **51**, 3–19.

MASUDA, T. & ANDO, S. 1988. Viscous flow around a rigid spherical body: A hydrodynamical approach. *Tectonophysics*, **148**, 337–346.

MERCIER, J. C. C. ANDERSON, D. A. & CARTER, N. L. 1977. Stress in the lithosphere. Inferences from steady state flow of rocks. *Pure and Applied Geophysics*, **115**, 199–226.

MEANS, W. D. 1981. The concept of steady state foliation. *Tectonophysics*, **78**, 179–199.

MITRA, S. 1978. Microscopic deformation mechanisms and flow laws in quartzites within the south anticline. *Journal of Geology*, **86**, 129–152.

ORD, A. & CHRISTIE, J. M. 1984. Flow stresses from microstructures in mylonitic quartzites from the Moine Thrust Zone, Assynt area, Scotland. *Journal of Structural Geology*, **6**, 639–654.

PATERSON, M. S. & LUAN, F. C. 1990. Quartz rheology under geological conditions. *This volume*.

POIRIER, J. P. 1985. *Creep of crystals*. Cambridge University Press.

PRICE, G. 1978. Study of the heterogenous fabric and texture within a quartz-feldspar mylonite using the photometric method. *Geological Society of America Bulletin*, **89**, 1359–1372.

PRIOR, D. J. 1988. *Deformation processes in the Alpine Fault Mylonites, South Island, New Zealand*. PhD Thesis, University of Leeds.

—— 1989. Deformation processes in the Alpine Fault Mylonites, South Island, New Zealand: *New Zealand Journal of Geology and Geophysics*, **31**, 526.

ROSS, J. V., AVE LALLEMENT, H. G. & CARTER, N. L. 1980. Stress dependence of recrystallized grain and subgrain size in olivine. *Tectonophysics*, **70**, 39–61.

SIBSON, R. H., WHITE, S. H. & ATKINSON, B. K. 1979. Fault rock distribution and structure within the Alpine Fault Zone: A preliminary report: *In*: WALCOTT, R. I. & CRESSWELL, M. M. (eds) *Origin of the Southern Alps*. Bulletin of the Royal Society of New Zealand, **18**, 55–65.

TAKEUCHI, S. & ARGON, A. S. 1976. Steady state creep of single phase crystalline matter at high temperatures. *Journal of Material Science*, **11**, 1542–1566.

TWISS, R. J. 1977. Theory and applicability of a recrystallized grainsize palaeopiezometer. *Pure and Applied Geophysics*, **115**, 227–244.

—— 1986. Variable sensitivity piezometric equations for dislocation density and subgrain diameter and their relevance to olivine and quartz. *American geophysical Union, Geophysical Monograph*, **36**, 247–263.

WALCOTT, R. I. 1984. Reconstruction of the New Zealand region for the Neogene. *Palaeogeography, Palaeoclimatology, Palaeoecology*, **46**, 217–231.

WELLMAN, H. W. 1979. An uplift map for the South Island of New Zealand and a model for the uplift of the Southern Alps: *In*: WALCOTT, R. I. & CRESSWELL, M. M. (eds) *Origin of the Southern Alps*. Bulletin of the Royal Society of New Zealand, **18**.

WHITE, S. H. 1984. Brittle deformation within ductile fault zones. *Proceedings 27th International Geological Congress*, **7**, 327–350.

——, BURROWS, S. E., CARRERAS, J., SHAW, M. D. & HUMPHREYS, F. J. 1980. On mylonites in ductile shear zones. *Journal of Structural Geology*, **2**, 175–187.

——, DRURY, M. R., ION, S. E. & HUMPHREYS, F. J. 1985. Large strain deformation studies using polycrystalline magnesium as a rock analogue, part I: Grainsize palaeopiezometry in mylonite zones. *Physics of the Earth and Planetary Interiors*, **40**, 201–207.

WHEELER, J. 1987. The significance of grain-scale stresses in the kinetics of metamorphism. *Contributions to Mineralogy and Petrology*, 17, 397–404.

WINTSCH, R. P. & KNIPE, R. J. 1983. Growth of a zoned plagioclase porphyroblast in a mylonite. *Geology*, **11**, 360–363.